International Research Journal of Engineering and Technology (IRJET) e-ISSN: 2395-0056
Volume: 10 Issue: 06 | Jun 2023 www.irjet.net p-ISSN: 2395-0072

Design of 3x6 axial-slot array antenna on circular cylinder waveguide for 2.45 Ghz IOT applications

Traore Seydou [1], Ouattara Yelakan Béranger[2], Siaka Fofana[3], Silue Dozohoua[4]

[1]*Department of Sciences of the Structures of Material and Technology (SSMT), Technology Labs, Felix Houphouet Boigny university, Abidjan, Ivory Cost*
[2]*Department of Sciences of the Structures of Material and Technology (SSMT), Technology Labs, Felix Houphouet Boigny university, Abidjan, Ivory Cost*
[3]*Department of Sciences of the Structures of Material and Technology (SSMT), Technology Labs, Felix Houphouet Boigny university, Abidjan, Ivory Cost*
[4]*Department of Technological Resources, African School of Information Technology and Communication (ESATIC), Abidjan, Ivory Cost*

Abstract - *In this paper, a rectangular slot array antenna has been designed on a circular cylinder, shorted at both ends and fed by TE11 mode. The antenna operating at the frequency of 2.45GHz is proposed for a radio frequency identification (RFID) reader. RFID along with Zigbee, Bluetooth, and WIFI are connectivity technologies for Internet of Things (IoT) networks. RFID technology is especially efficient for the detection of objects in the near field. Thus, the results of the simulations performed with the theoretical method EC-FDTD under Matlab software, were compared with those obtained with the commercial software HFSS and the practical measurements. The array antenna consisting of 3x6 rectangular axial slots was realized and its S11 parameter was measured. The results of the practical measurements are in accordance with the numerical results. The antenna has a high gain of about 10 dBi, and a good reflection coefficient -25 dB at the frequency of 2.45 GHz. Furthermore, the mapping and evolution of the electric field determined at 10 cm from the antenna, shows that this antenna generates a strong and uniform electric field in the near field area around the cylinder. Therefore, this antenna can be used to ensure capacitive coupling and good communication between the reader antenna and the tag.*

Key Words: Array antennas, Slot waveguide, Circular cylindrical, Omnidirectional, Internet-of-things (IoT), Near field.

1. INTRODUCTION

To monitor physical objects when they are stable or in motion in various fields such as healthcare, urban infrastructure, transportation and energy, the Internet of Things (IOT) uses various technologies including radio frequency identification (RFID).

Thus, to meet various requirements with better identification performance, many types of RFID systems are rapidly emerging. These include low frequency (LF, 125-134 KHz), high frequency (HF, 13.56 MHz) and ultra-high frequency (UHF, 860-960 MHz and 2.4 GHz). Currently, passive near-field RFID-UHF technology operating by inductive coupling is receiving a lot of attention for near-field identification as it brings several improvements compared to low and high frequency RFID (LF/HF). Indeed, the detection speed and the volume of data exchanged are higher in UHF than in HF, the manufacturing cost of the tags is significantly lower than that of HF tags. But UHF RFID can also operate in the near field through the electric field (capacitive coupling) and communicate in the far field through electromagnetic waves (EM). One of the limitations of current RFID systems is that they do not work well at close range (near field). This near-field communication problem is due to an insufficient magnetic field produced by the antenna of the reader and tag in UHF as well as poor impedance matching at the tag.

It is therefore important to design new antennas that can function properly in these near-field communications. Several works dealing with near and far field antenna design have been published [1]-[2] and have focused on the inductive coupling between the reader and the tag antenna via the magnetic field. In order to solve the above problems, the configuration of a 3x6 slot array antenna cut on a cylindrical waveguide is studied. It is fed in TE11 mode at a frequency of 2.45 GHz.

Indeed, an array of rectangular slots cut in the wall of a hollow cylinder seems to be a good configuration for omnidirectional radio coverage: it is less expensive, simple to build and has almost no losses when fed by a monopole. Research and publications on circular slot waveguides date from the 1950s to the present day [3]-[11]. The study of radiation from an axial slot onto a cylindrical conductor has been widely published [4]-[6]. However, the papers [12]-[14] focus on arrays of axial and circumferential slits linearly arranged on the cylindrical generator. Most of these antenna characterisations are simulated on commercial software such as HFSS or CST [14], [24]-[25].

The first mention of the EC-FDTD (Equivalent-Circuit Finite Difference Time Domain) method appears, to our knowledge,

in the publications of Gwarek et al [18] and Craddock et al [19]. The first implementations of the proposed EC-FDTD algorithm were made for a regular Cartesian mesh, as described in [20]-[21] and in more detail in [22]-[23]. Following Maxwell's equations, the appropriate EC-FDTD formulation is directly deducible from its differential form (which is certainly constitutive of the conventional FDTD scheme) or from its integral form, the latter defining the starting point of our EC-FDTD scheme. This method has never been used for modelling cylindrical waveguide slotted antennas. The proposed antenna configuration is based on an array of axial slots arranged linearly or non-linearly along the length. It consists of six (6) rings of three slots each, i.e. eighteen (18) slots in total (see Figure 1). Indeed, the advantage of three (03) slots placed at 120° from each other on the same ring (or level) allows us to theoretically cover the desired 360°, to increase the number of antennas (slots) of the array and therefore of radiating elements and to reduce the size (height) of the cylinder.

2. MATERIALS AND METHODS

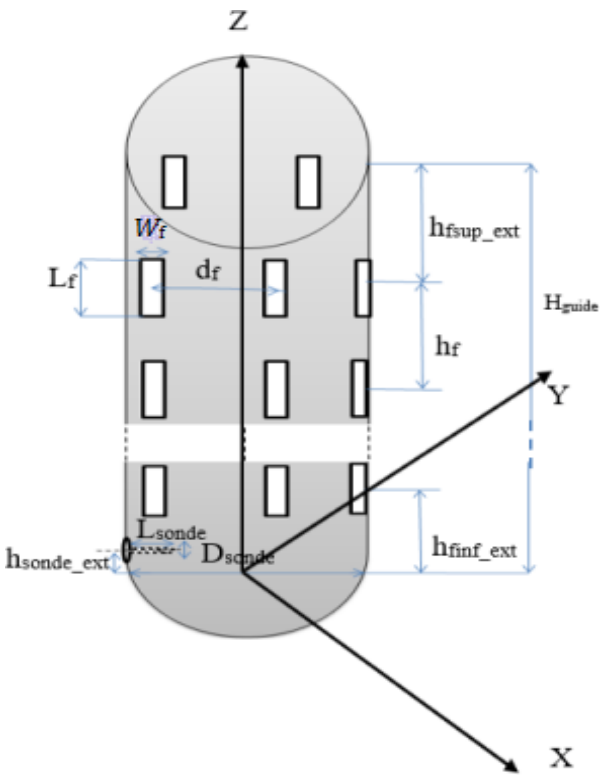

Fig-1: General configuration of a slotted cylindar waveguide antenna

The general structure Figure 1 of the proposed configuration is a cylindrical guide of circular section of height (Hguide,); radius guide (r_{guide}) and thickness.
The array of radiating antennas shaped on the surface of the short-circuited cylinder at both ends is a set of small rectangular axial slots of length $\left(L_f = \lambda_0/4\right)$ and wide $\left(w_f = L_f/10\right)$. In the direction of the axis, several slots are spaced each other by $\lambda_g/2$. The first slot, located at the bottom of the cylinder is about $h_{f\,in\,ext} = 3\times\lambda_g/4$ compared with the lower end of the cylinder. While the last slot is at the top of $h_{f\,\sup\_ext} = \lambda_g/4$ compared with the top end of the cylinder. At each crown (or ring), there are several slots spaced from $d_f = r_{guide}.(\theta_n - \theta_{n-1})$ or θ_{fn} representing the angular difference in radian between two successive slots and θ_1 for the angular position of the first slot.
Equivalent-Circuit *(*EC) FDTD has several advantages over the classic FDTD. Since its update values are voltages and currents (as opposed to electric and magnetic fields), it allows an easy integration of electronic components, such as for instance diodes and transistors, into the simulation. In addition, it provides increased computational speed thanks to a reduced number of multiplications in the update equations [24]-[26]. Finally, it may be generalized to arbitrary dispersive media.

OpenEMS is a free source code used for the rigorous modeling of the electromagnetic field (EM) under Matlab or octave [15]. It is based on the equivalent circuit of finite-difference time-domain method (FDTD). The program designer is rigorously placed in the Matlab environment structure and its mesh. The mesh step selection appears especially important to get a good result. It is possible to visualize the structure from the AppCSXCAD graphical interface associated with Matlab. The basic EC-FDTD equations are based on the classical FDTD. We have:

$$\oint_A \vec{H}\times\vec{ds} = +\frac{d}{dt}\iint_A \varepsilon\vec{E}\times\vec{dA} + \iint_A \kappa\vec{E}\times\vec{dA} \quad (1)$$

$$\oint_A \vec{E}\times\vec{ds} = -\frac{d}{dt}\iint_A \mu\vec{H}\times\vec{dA} - \iint_A \sigma\vec{H}\times\vec{dA} \quad (2)$$

The discretisation from the YEE scheme [14] leads to:

$$H_y\Delta_y - H_y\left(n_z - 1\right)\Delta_y - H_z\Delta_z + H_z\left(n_y - 1\right)\Delta_z \approx \tilde{A}_X\left(\varepsilon\frac{d}{dt}E_X + \kappa E_X\right) \quad (3)$$

$$E_y\Delta_y - E_y\left(n_x + 1\right)\Delta_y - E_x\Delta_x + E_x\left(n_y + 1\right)\Delta_x \approx -\tilde{A}_z\left(\mu\frac{d}{dt}H_z + \sigma H_z\right) \quad (4)$$

Where we have the voltage and current components as following:

$$\upsilon_x = E_x\Delta_x, \quad \upsilon_y = E_y\Delta_y, \quad \upsilon_z = E_z\Delta_z$$
$$i_x = H_x\Delta x, \quad i_y = H_y\Delta_y, \quad i_z = H_z\Delta_z$$

Then, equations (3) and (4) become:

$$i_y - i_y\left(n_z - 1\right) - i_z + i_z\left(n_y - 1\right) \approx C_x\frac{d}{dt}\upsilon_x + G_x\upsilon_x \quad (5)$$

With:

$$C_x = \frac{\varepsilon A_x}{\Delta_x} \qquad G_x = \frac{\kappa A_x}{\Delta_x}$$

And :

$$\upsilon_y - \upsilon_y\left(n_x + 1\right) - \upsilon_x + \upsilon_x\left(n_y + 1\right) \approx -L_z\frac{d}{dt}i_z - R_z i_z \quad (6)$$

With :

$$L_z = \frac{\mu A_z}{\Delta x} \qquad R_z = \frac{\sigma A_z}{\Delta x}$$

The voltages and currents are sampled respectively on the time $n_t\Delta_t$ and $\left(n_t + 0,5\right)\Delta_t$. We obtain equations (7) and (9). This The voltages and currents are sampled respectively on the time $n_t\Delta_t$ and $\left(n_t + 0,5\right)\Delta_t$. We obtain equations (7) and (9). This yield update equation for, the voltage υ_X in equation (8) and the current i_y in equation (10):

$$\upsilon_x^{n_t} = \frac{2C_x - \Delta_t G_x}{2C_x + \Delta_t G_x}\upsilon_x^{n_t-1} + \frac{2\Delta_t}{2C_x + \Delta_t G_x} \times \left(i_y^{n_t-0,5} - i_y^{n_t-0,5}\left(n_z - 1\right) - i_z^{n_t-0,5} + i_z^{n_t-0,5}\left(n_y - 1\right)\right) \quad (7)$$

$$\upsilon_y^{n_t} - \upsilon_y^{n_t}\left(n_x + 1\right) - \upsilon_x^{n_t} + \upsilon_x^{n_t}\left(n_y + 1\right) = L_z\frac{i_y^{n_t+0,5} - i_y^{n_t-0,5}}{dt} + R_z\frac{i_y^{n_t+0,5} + i_y^{n_t-0,5}}{2} \quad (8)$$

$$i_y^{n_t-0,5} - i_y^{n_t-0,5}\left(n_z - 1\right) - i_z^{n_t-0,5} + i_z^{n_t-0,5}\left(n_y - 1\right) = C_x\frac{\upsilon_x^{n_t} - \upsilon_x^{n_t-1}}{\Delta t} + G_x\frac{\upsilon_x^{n_t} + \upsilon_x^{n_t-1}}{2} \quad (9)$$

$$i_y^{n_t+0,5} = \frac{2L_z - \Delta_t R_z}{2L_z + \Delta_t R_z}i_y^{n_t-0,5} - \frac{2\Delta_t}{2L_z + \Delta_t R_z} \times \left(\upsilon_y^{n_t} - \upsilon_y^{n_t}\left(n_x + 1\right) - \upsilon_x^{n_t} + \upsilon_x^{n_t}\left(n_y + 1\right)\right) \quad (10)$$

When we apply the contour path model of the narrow slot [26] within the slots air gap, we obtain equation (11) derived from equation (3).

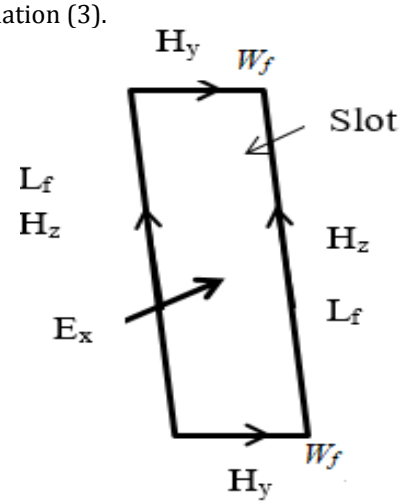

Fig-2: Ampère's law for *E*

$$H_y w_f - H_y\left(n_z - 1\right)w_f - H_z L_f + H_z\left(n_y - 1\right)L_f \approx \tilde{A}_S\left(\varepsilon_0\frac{d}{dt}E_x\right) \quad (11)$$

$A_s = L_f \times w_f$ is the slot surface

The electromagnetic field in the slot are calculated by the expressions (12):

$$E_x^{n_t} = E_x^{n_t-1} - \frac{\Delta t}{\varepsilon_0\tilde{A}_s} \times \begin{bmatrix} \left(H_y^{n_t-0,5} - H_y^{n_t-0,5}\left(n_z - 1\right)\right) \times w_f \\ -\left(H_z^{n_t-0,5} - H_z^{n_t-0,5}\left(n_y - 1\right)\right) \times L_f \end{bmatrix} \quad (12)$$

Finally, the TE11 mode is obtained inside the cylinder [15] by combining electric and magnetic fields E_x, E_y, H_x, H_y , wrote according to radial and orthoradial fields $E_\rho, E_\phi, H_\rho, H_\phi$ (These are the field components inside the waveguide):

$$E_\rho = \frac{-j\omega\mu}{k_c^2\rho}A\cos\left(\phi\right)J_1\left(k_c\rho\right)e^{-j\beta z} \quad (13)$$

$$E_\phi = \frac{-j\omega\mu}{k_c}A\sin\left(\phi\right)J_1'\left(k_c\rho\right)e^{-j\beta z} \quad (14)$$

$$H\rho = \frac{-j\beta}{k_c}A\sin\left(\phi\right)J_1'\left(k_c\rho\right)e^{-j\beta z} \quad (15)$$

$$H_\phi = \frac{-j\beta}{k_c^2\rho}A\cos\left(\phi\right)J_1\left(k_c\rho\right)e^{-j\beta z} \quad (16)$$

Where:

J_1 : The Bessel function of first kinds,

$J_1^{'}$: Refers to the derivative of J_1

The electrical parameters of the proposed antenna are calculated base on the transmission line theory. The amplitude of the reflected voltage (v_{ref}) wave normalized to the amplitude of the incident voltage (v_{inc}) wave is defined as the voltage reflection coefficient, S_{11}:

$$S_{11} = \frac{v_{ref}}{v_{inc}} \quad (17)$$

With:

$$V_{ref} = V - V_{inc} \quad (18)$$

$$v_{inc} = \frac{1}{2}\left(v + i * Z_{TE}\right) \quad (19)$$

$$i_{inc} = \frac{1}{2}\left(i + \frac{v}{Z_{TE}}\right) \quad (20)$$

v : Total voltage in the waveguide antenna
i : Total current in the waveguide antenna

Equation (17) can be expressed in another form:

$$S_{11} = \frac{V - V_{inc}}{V_{inc}} = \frac{V - \frac{1}{2}\left(V + i * Z_{TE}\right)}{\frac{1}{2}\left(V + i * Z_{TE}\right)} = \frac{\left(V - i * Z_{TE}\right)}{\left(V + i * Z_{TE}\right)} \quad (21)$$

Z_{TE} is the wave impedance that relates the transverse electric and magnetic fields:

$$Z_{TE} = \frac{E_\rho}{H_\phi} = -\frac{E_\phi}{H_\rho} = \frac{z_0 . k}{\beta} \quad (22)$$

z_0 and k represent respectively the intrinsic impedance and the wave number in air material filling the waveguide.

k_c : Cut off Waves Numbers

$$k_c = \frac{p_{11}^{'}}{a}$$

$$\beta = \sqrt{k^2 - \left(\frac{p_{11}^{'}}{a}\right)^2}$$

Where:

$p_{11}^{'}$: Is the first root of $J_1^{'}$

we put the current i as a factor in expression (18) and then simplify, we obtain the expression:

$$S_{11} = \frac{\left(Z_{11} - Z_{TE}\right)}{\left(Z_{11} + Z_{TE}\right)} \quad (23)$$

With:

$$Z_{11} = \frac{v}{i} \quad (24)$$

Where, Z11 is the Circuit input impedance

3. Results and Discussion

3.1. Simulation of different configurations under EC-FDTD

First, the antenna is modelled with EC-FDTD method programmed on the Matlab software for four configurations of slots as presented in Figure 2:

1) One slot
2) one ring of three slots;
3) two rings of three slots;
4) Six rings of three slots.

The results of simulations are used to find the optimum configurations of slots on the cylindrical cavity antenna in frequency band 2.45 GHz (i.e., high gain, bandwidth and return loss etc.). Then we compared the simulated parameters with HFSS results.

In Table 1, the values of the various parameters used for the antenna geometry are recorded.

Figure 3 and Figure 4 respectively show the S11 parameter simulation's results and of the radiation pattern of the different antennas.

Table 1. Dimensions of the proposed antenna

Antenna parameters	One slot	One ring	Two rings	Six rings
Cavity radius(mm)	58	56	56	57
Cavity lenght(mm)	135.85	229.75	305.95	645.95
Slot lenght(mm)	62.5	57.5	57.5	57.5
Slot width(mm)	6.25	5.75	5.75	5.75

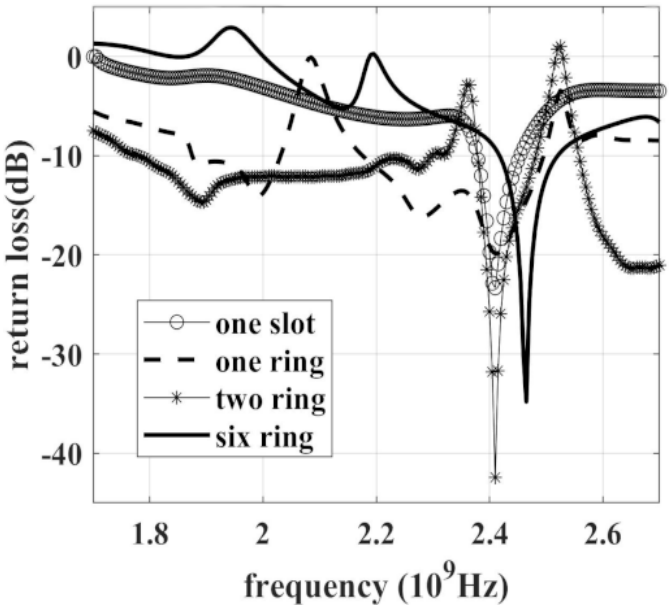

Fig-3: S11 simulation of four types of cylinder antenna configuration simulated with EC-FDTD

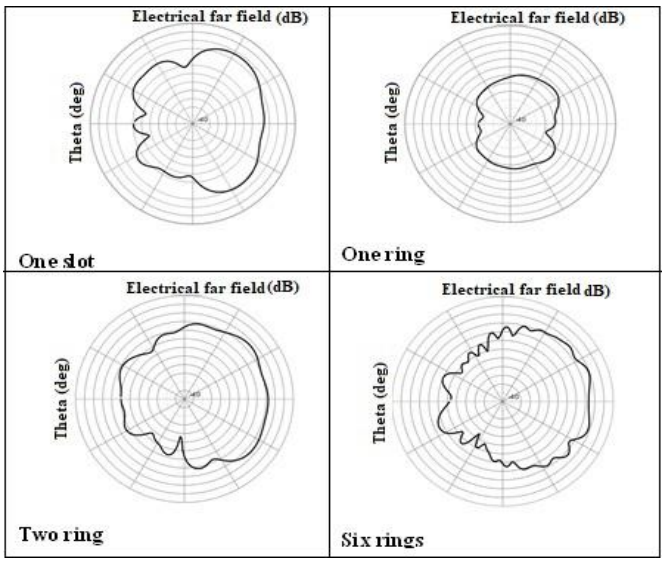

Fig-4: Radiation pattern 2D for different slots configurations simulated with EC-FDTD

The S11 characteristics and radiation patterns of different configurations have been simulated with the EC-FDTD source code.

The results of these simulations allowed us to determine the bandwidths of these different antennas at -10dBi which have been recorded in Table 2.

The increase in the number of slots systematically leads to an increase in the size of the antenna (we went from 135.85mm length for the one slot antenna to 645.95mm for the 18 slot antenna). Therefore, the manual adaptation of the mesh size for each simulation does not allow us here to appreciate the effect of the increase of the slots on the bandwidth. But these results show that these antennas can indeed operate at the 2.45GHz frequency.

Concerning the radiation patterns, the simulation results are in agreement with our assumptions. Their quasi-omnidirectional nature for the antenna arrays as shown in figure 2 will allow us to cover the 360°. Nevertheless, we can always increase the number of slots on the crowns to improve this result.

Table 2. Characteristics of the differents antennas configurations

Slot ring	Bandwidth	Return loss
One slot	3%	-11dB at 2.45Ghz
One ring	13%	-16.42dB at 2.45Ghz
Two rings	2.71%	-15.48dB at 2.45Ghz
Six rings	4.2%	-18.81dB at 2.45Ghz

3.2. Comparative Study

In this section, we have computed the antenna structure and simulated under Matlab using openEMS source code that uses finite difference theory (EC-FDTD) as modeling method of the electromagnetic field.

The parameters considered for the structure geometry are those of table 1, more precisely those of six rings of slots resulting to eighteen (18) slots in total. The slots are well aligned by number of six (06) on each angular position. Figure 5(a) and Figure 5(b) show the numerical configurations and Figure 5(c) shows the picture of the antenna made of aluminum. The slots were obtained with an automatic machine of high precision. The folding machine made possible to obtain the rounded shape and the waveguide is shorted manually.

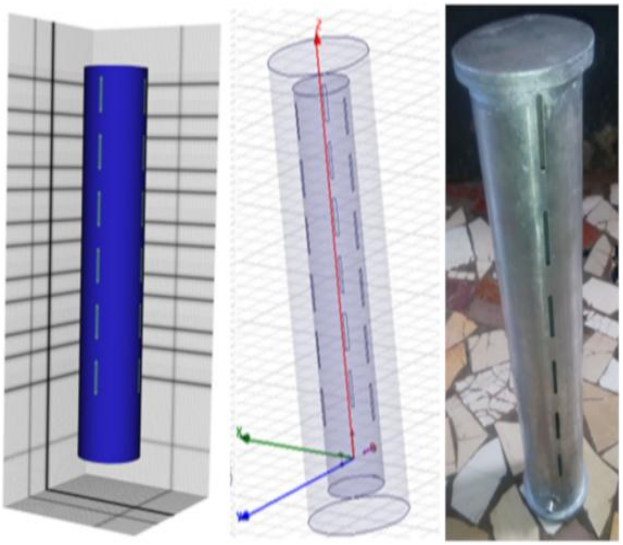

Fig-5: Proposed cylinder antenna: (a) antenna structure programmed with EC-FDTD, (b) antenna structure designed with HFSS and (c) antenna structure made with aluminum.

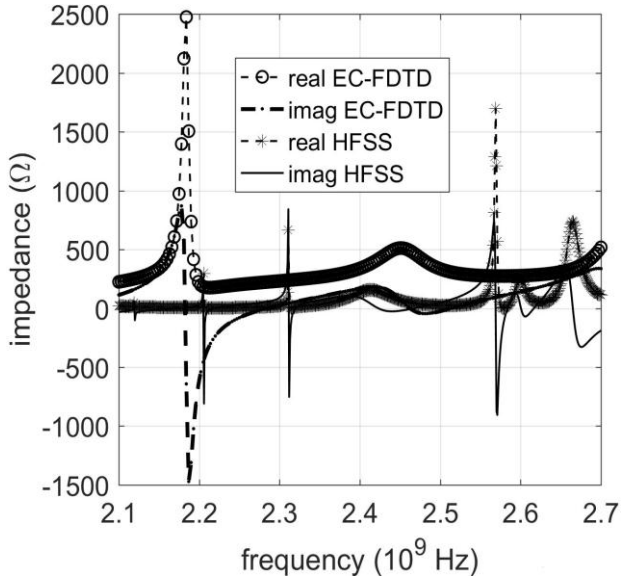

Fig-6: Simulated input impedance for the proposed antenna with HFSS and EC-FDTD

Figure 6 shows that at the resonant frequency of 2.45 GHz, the input resistance is about 50 Ω while the reactance is zero, which is ideal for the choice of the matching point.

The Keysight reference instrument N9330B operating in the frequency range at 25 MHz- 4GHz, allowed us to realize the practical measures of the reflection feedback S11. The result of these measurements is compared to the numerical results in Figure 7.

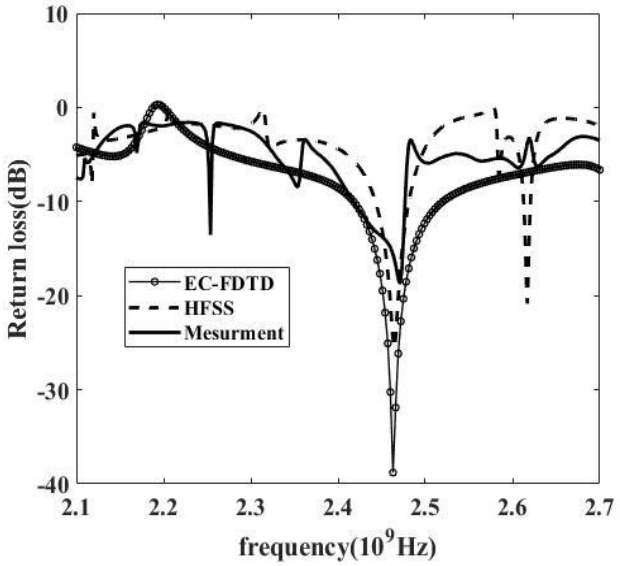

Fig-7: Comparison between simulated and measured return loss (S11).

The simulation results presented in Figure 7 show that the curve obtained from EC-FDTD offers a wider bandwidth than that obtained with HFSS and seems to be more in agreement with the practical measurement. The observed gap between numerical results and practical measures are certainly due to manufacturing defects.

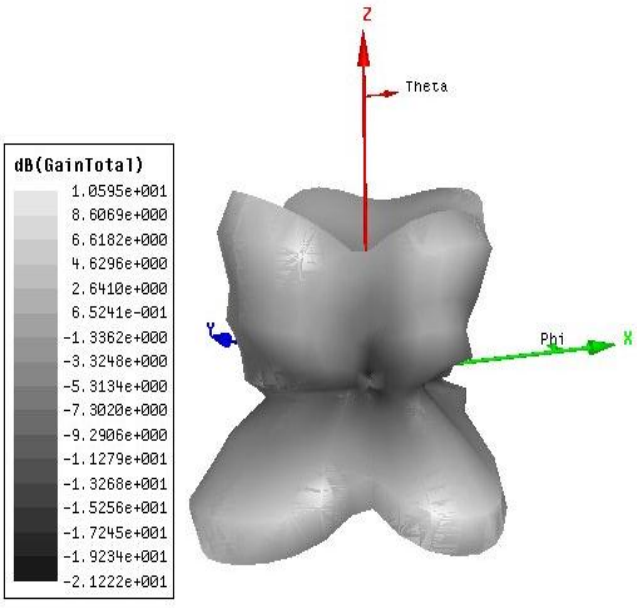

Fig-8: 3D Radiation pattern simulated with HFSS.

Figure 8 shows the 3D radiation pattern of our simulated antenna on HFSS. We can see the field distribution with a gain level of more than 10dB.

3.3. *Near field survey for IOT (Internet of Things) applications*

This study aims at evaluating the electric field characteristics in a 10cm area around the antenna. Thus, we could obtain:
- The electric field mapping(fig-9) at a height of 10cm above the antenna,

- The linear evolution curve of the E field over a distance of 10cm (fig-10).

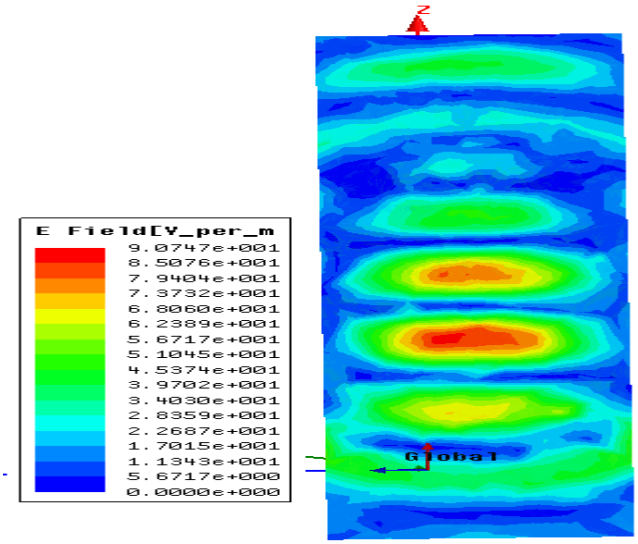

Fig-9: Near-field distribution of the reader antenna

The electric field mapping obtained at a height of 10 cm above the array antenna, shows a reading area of 64. (L)×34 (W) cm² which is favorable for the detection of dipole type tags by capacitive coupling.

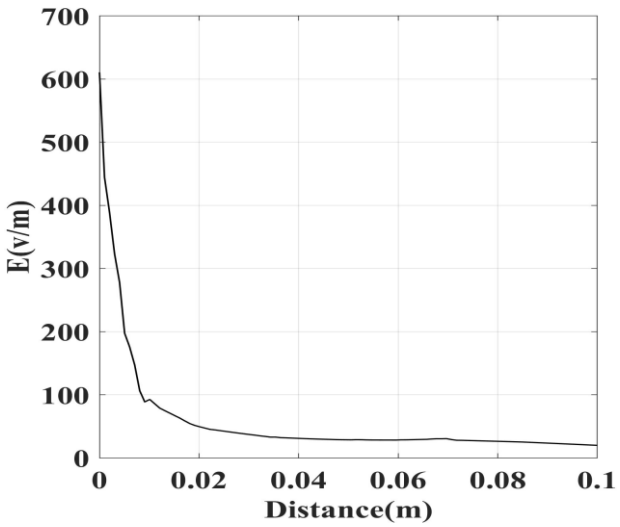

Fig-10: Evolution of the electric field over the antenna array as a function depending on the distance

This curve shows that the electric field decreases progressively as one moves away from the antenna. There are two parts as far as the evolution of this curve is concerned:

- Between [0 ;1cm] it decreases very quickly from 600 v/m to 100v/m
- Between [1cm ;10cm] it decreases very slowly and is practically constant beyond 3cm with an approximate value of 25V/m.

he mapping of the electric field and its evolution over a distance of 10 cm shows a good distribution of the electric field in the near field area.

4. CONCLUSION

In this study, we have characterized circular cylindrical waveguide antennas consisting of an array of rectangular axial slots using three different methods. These are two numerical electromagnetic field modelling methods (HFSS and EC-FDTD) and practical measurements performed on a fabricated prototype antenna. The size and particular location of the annular slots on the waveguide contour seem to be very important for obtaining optimal results. It was possible to observe an increasing gain of the antenna with the number of annular slots.

But at the same time, there is a narrowing of the bandwidth which can be increased by choosing not to align the resonance of all components (slots) of the same column on one point, but on several. Furthermore, the practical results, consistent with the numerical results, show that the omnidirectional antenna can operate with good gain in the 2.4GHz frequency band. Also, the electric field mapping obtained at à distance of 10cm from the antenna shows a good electric field distribution in the near field area. Therefore, this array antenna based on capacitive couplings for near-field RFID applications can be used for goods tracking or supply chain management. But it can also communicate in the far field by means of electromagnetic (EM) waves.

REFERENCES

[1] B. Shrestha, A. Elsherbeni, L. Ukkonen, "UHF RFID Reader Antenna for near-field and far-field operations," *IEEE Antennas Wireless Propag. Lett, vol.10, Nov.2011, pp. 1274-1277.*

[2] X. Qing, C. Khan Goh, Z. Ning Chen, " A broadband UHF near-field RFID Antenna," *IEEE Trans. Antennas Propag., vol.58, no.12, Dec.2010, pp. 3829-3838.*

[3] G. Sinclair, "The Patterns of Slotted-Cylinder Antennas," *Proc. IRE, Vol. 36, pp.1487-1492, Dec. 1946*.

[4] S. Silver and W. K. Saunders, "The External Field Produced by a Slot in an Infinite Circular Cylinder," *Jour. Appl. Phys. Vol. 21, pp. 745-749, Aug. 1950.*

[5] L. L. Bailin, "The radiation field produced by a slot in a large circular cylinder," *IEEE Trans. Antennas Propag., vol.3, no.3, pp.128–137, Jul. 1955*

[6] S. Sensiper, W. G. Sterns, and T. T. Taylor (1952), "A further study of the patterns of single slots on circular conducting cylinders," *Trans. IRE Prof. Group Antennas Propag, 3(1), 240–250.*

[7] J. R. Wait, "Electromagnetic Radiation from Cylindrical Structures", *Pergamon Press, Inc., New York, NY, 1959*.

[8] E. W. Wolff, Antennas Analysis, *John Wiley & Sons, Inc., USA, 1966.*

[9] S. W. Lee and S. Safavi-Naini, "Asymptotic solution of surface field due to a magnetic dipole on a cylinder," *University of Illinois at Urbana-Champaign, Electromagnetics Laboratory Report n°. 76-11, 1976.*

[10] S. W. Lee, S. Safavi-Naini, and R. Mittra, "Mutual admittance between slots on a cylinder," *University of Illinois at Urbana-Champaign, Electromagnetics Laboratory Report n°. 77-8, 1977.*

[11] G. E. Stewart and K. E. Golden, "Mutual admittance for axial rectangular slots in a large conducting cylinder," *IEEE Trans. Antennas Propagat., vol. AP-19, pp. 120-122, 1971.*

[12] L. Shafai. and E. M. Hassan (1981), "Field distribution and radiation field of finite axial slots on circular waveguides," IEE *Proc. Part H Microwaves Opt. Antennas, 128(5), 263–267.*

[13] D. H. Shin and H. J. Eom (2005), "Radiation from narrow circumferential slots on a conducting circular cylinder," IEEE Trans. Antennas Propag., 53(6), 2081–2088.

[14] D. H. Shin and H. J. Eom (2006), "Radiation from narrow axial slots on a conducting circular cylinder," *Radio Sci., 41, RS4005,* doi: 10.1029/2005RS003430

[15] L. Thorsten, R. Andreas, H. Sebastian and E. Daniel, "openEMS – a free and open-source equivalent-circuit (EC) FDTD simulation platform supporting cylindrical coordinates suitable for the analysis of traveling wave MRI applications," *Int. J. Numer. Model. 2012,* doi: 10.1002/jnm.1875

[16] A. Taflove, S. Hagness, "Computational Electrodynamics: The Finite difference Time-domain Method," *3rd edn. Artech House: Norwood, MA, 2005*.

[17] M.D. Pozar, *Microwave Engineering 4th edn*, John Wiley &1ps03-vidmar

[18] W.K. Gwarek, "Analysis of an arbitrarily-shaped planar circuit – a time-domain approach," *IEEE Transactions Microwave Theory and Techniques 1985; MTT 33(10):1067–1072*.

[19] I.J. Craddock, C.J. Railton and J.P. McGeehan. "Derivation. and application of a passive equivalent circuit for the finite difference time domain algorithm,'' *IEEE Microwave and Guided Wave Letters 1996; 6(1):40–42*

[20] A. Lauer, I. Wolff, "Stable and efficient ABCs for graded mesh FDTD simulations," *IEEE MTT-S International Microwave Symposium Digest, Vol. 2, Baltimore, MD, 1998; 461–464.*

[21] A. Lauer, I. Wolff, "A conducting sheet model for efficient" wide band FDTD analysis of planar waveguides and circuits," *IEEE MTT-S International Microwave Symposium Digest, Vol. 4, Anaheim, CA, 1999; 1589–1592,* doi:10.1109/MWSYM.1999. 780262.

[22] A. Rennings, A. Lauer, C. Caloz, I. Wolf. "Equivalent Circuit (EC) FDTD Method for Dispersive Materials: Derivation, Stability Criteria and Application Examples," *Springer Proceedings in Physics, vol. 121. Springer-Verlag: Berlin, 2008; 211–238.*

[23] A. Rennings, "Elektromagnetische zeitbereichssimulationen innovativer antennen auf basis von metamaterialien," PhD Thesis, University of Duisburg-Essen, September 2008.

[24] I.I. Ahmed, A.E. Taha "A cylindrical wideband slotted patch antenna loaded with Frequency Selective Surface for MRI applications". *Engineering Science and Technology, an International Journal 20 (2017) 990–996*

[25] R. Joseph, S. Nakao, and T. Fukusako, "Circcular slot antennas using L-shape probe for broadbande circular polarization," *Progress in Electromagnetics Research C, Vol. 18, 153-168, 2011*

[26] A. Rennings, S. Otto, A. Lauer, C. Caloz, and P. Waldow. "An extended equivalent circuit based FDTD scheme for the efficient simulation of composite right/left-handed metamaterials," Proc. of the Euro. Microw. Assoc., vol. 2, no. 1, pp. 71–82, March 2006.

[27] A. Rennings, S. Otto, C. Caloz, A. Lauer, W. Bilgic, and P. Waldow. "Composite right/lefthanded extended equivalent circuit (CRLH-EEC) FDTD: stability, dispersion analysis with examples," Int. J. Numer. Modell., vol. 19, no. 2, pp. 141–172, March 2006.

[28] Taflove, A., K. R. Umashankar, B. Beker, F. Harfoush, and K. S. Yee, "Detailed FDTD analysis of electromagnetic fields penetrating narrow slots and lapped joints in thick conducting screens,"*IEEE Trans. Antennas Propagat., Vol. 36, 1988, pp. 247-257.*